

Article

# ICA and ANN Modeling for Photocatalytic Removal of Pollution in Wastewater

Sina Razvarz  and Raheleh Jafari \*

Departamento de Control Automatico CINVESTAV-IPN (National Polytechnic Institute), Mexico City 07360, Mexico; srazvarz@yahoo.com

\* Correspondence: rjafari@ctrl.cinvestav.mx; Tel.: +52-555-149-7434

Received: 28 June 2017; Accepted: 20 July 2017; Published: 11 August 2017

**Abstract:** This paper discusses the elimination of Colour Index Acid Yellow 23 (C.I. AY23) using the ultraviolet (UV)/Ag-TiO<sub>2</sub> process. To anticipate the photocatalytic elimination of AY23 with the existence of Ag-TiO<sub>2</sub> nanoparticles processed under desired circumstances, two computational techniques, namely artificial neural network (ANN) and imperialist competitive algorithm (ICA) modeling are developed. A sum of 100 datasets are used to establish the models, wherein the introductory concentration of dye, UV light intensity, initial dosage of nano Ag-TiO<sub>2</sub>, and irradiation time are the four parameters expressed in the form of input variables. Additionally, the elimination of AY23 is considered in the form of the output variable. Out of the 100 datasets, 80 are utilized in order to train the models. The remaining 20 that were not included in the training are used in order to test the models. The comparison of the predicted outcomes extracted from the suggested models and the data obtained from the experimental analysis validates that the performance of the ANN scheme is comparatively sophisticated when compared with the ICA scheme.

**Keywords:** artificial neural network; experimental data; modeling; particle swarm optimization; pollutant

## 1. Introduction

Developed countries are facing a serious problem of water pollution caused by dyes. Synthetic dyes are significant water contaminants and industrial pollutants. Azo dyes, the greatest class of synthetic dyes utilized in the food industry, are specified by the appearance of one or more azo bonds  $-N=N-$  on par with one or more aromatic systems. In general, these dyes cannot be eliminated by conventional water treatment systems [1]. Hence, the elimination of dyes from wastewater has become a matter of concern for the relevant industries. The advancement of highly-efficient techniques for the removal of dangerous pollutants from air, soil, and water is one of the most active fields in environmental research [2].

Generally, the behavior associated with the photochemical system is quite complicated. Therefore, the advancement of reliable and robust predictive models is still required for the elimination of organic pollutants. Numerable modeling techniques based on artificial intelligence, like artificial neural networks (ANNs) and imperialist competitive algorithm (ICA) have appeared as adsorbent tools and have represented a better potential for modeling complicated systems [3–12]. The training of ANNs can be done with real data in order to take up issues related to complex and nonlinear problems where mathematical modeling may be too unsuitable or complicated. ANN is based on the minimization of the empirical risk which will compel the solution to be enclosed in a local minimum as well as over-fitting of the network [13].

In order to evaluate, as well as to locate, the superior candidates for a task, ICA is considered to be a very efficient methodology [14,15]. This algorithm imparts fewer mathematical needs, and it does

not need very accurate stated mathematical models. ICA is a novel global search scheme influenced by the socio-political process of imperialistic competition. Similar to other evolutionary types, ICA begins with an initial population. Population individuals, which are termed as the country considered to be of two types, namely, colonies and imperialists, that altogether form some empires [16].

Since very few studies have been done on the application of ANN and ICA in water sector [17], so the primary aim of this paper is the generalization of two techniques based on the ANN and ICA in order to estimate the elimination of Colour Index Acid Yellow 23 (C.I. AY23) by Ag-TiO<sub>2</sub> process. Here we investigate the photocatalytic proficiency of the Ag-TiO<sub>2</sub> particles for elimination of AY23 as a refractory pollutant. The outcome of usable prime factors to be mentioned as the initial dye concentration, ultraviolet (UV) light intensity, irradiation time, as well as the dosage of Ag-TiO<sub>2</sub> nanoparticles have been discussed. A few sets of data extracted from the literature are implemented, and the ANN and ICA methodologies are generalized on the basis of predictive models in order to eliminate AY23 in water by utilizing a set of chosen water quality criteria. Predictive potencies of the generalized models are verified by utilizing multiple statistical performance criteria parameters. Both ANN and ICA modeling methods display good predictions in this study. The ANN model is more precise when compared with ICA model. This paper is one of the first attempts in the developing of ANN and ICA modeling methods for the removal of AY23 in water by the UV/Ag-TiO<sub>2</sub> process.

## 2. Literature Survey

It has become a necessity for the development of highly-efficient techniques in order to eliminate organic pollutants by transforming them into less adverse compounds or by thorough mineralization [11]. Currently, chemical treatment techniques based on the generation of hydroxyl radicals, termed as advanced oxidation procedures (AOPs) have been expanded [1]. An intense study of TiO<sub>2</sub> as a photocatalyst has been conducted for the reason of its immense chemical stability, without any toxicity, low cost, and exquisite deterioration for organic pollutants [18]. The growth of UV/TiO<sub>2</sub> processes to attain entire mineralization associated with organic pollutants were investigated thoroughly for a broad variety of industrial dyes [19]. Heterogeneous photocatalysis through amalgamation of TiO<sub>2</sub> and UV light is considered as one of the promising AOPs for the devastation of water-soluble organic pollutants observed in water, as well as wastewater.

Activated carbon, as an absorbent, is popular for the removal of pollutants from wastewater. In [20] boosted regression trees and ANNs have been applied for modeling and optimization of methylene blue and Cd(II) removal from a binary aqueous solution by natural walnut carbon. Adsorption is a highly-proposed scheme for the removal of pollutants, such as dyes. A least squares-support vector machine, ANN, and the response surface method (RSM) have been proposed for modeling the facilitated adsorption of methylene blue dye [21]. The MnO<sub>2</sub>-nanoparticles, due to their high specific surface area, are suitable for pollutant removal. An ANN has been utilized for the precise prediction of percentages of brilliant green, crystal violet, and methylene blue dye removal from aqueous solutions using MnO<sub>2</sub>-NP-AC adsorbent [22]. The nano-adsorbents, by having high specific surface area and accessible surface adsorption sites, are more capable for the adsorption of pollutants. The  $\gamma$ -Fe<sub>2</sub>O<sub>3</sub> nanoparticle-loaded activated carbon is applied for the ultrasound-assisted simultaneous removal of dyes from aqueous solution, and the relative variable importance on adsorption in the batch system is studied using RSM and ANN [23]. A RSM and ANN have been utilized for removal of ternary toxic dyes onto copper sulfide nanoparticles loaded on activated carbon [24]. ANN and RSM have been proposed for modeling and interaction of the variables for the maximum removal percentage of ternary dyes utilizing the experimental data on the basis of the central composite design [25].

### 3. Materials and Methods

#### 3.1. Materials

Tetraisopropylorthotitanate  $\text{Ti}(\text{OC}_3\text{H}_7)_4$ , methanol (MeOH), as well as silver nitrate ( $\text{AgNO}_3$ ), were acquired from Merck (Darmstadt, Germany) and utilized without any additional purifications. AY23 was purchased from Acros (New York, USA) and utilized without additional purification. Figure 1 displays the chemical structure of this dye. Deionized water is employed throughout the work.

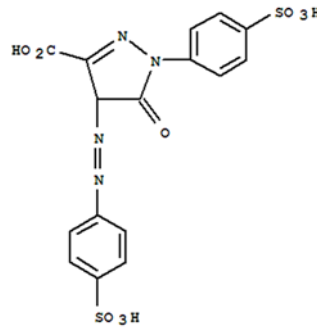


**Figure 1.** Chemical structure of Acid Yellow 23 (AY23).

#### 3.2. Analytical Technique

In the presence of  $\text{Ag-TiO}_2$ , AY23 is utilized as the pollutant. Sample solutions are sonicated before irradiation for 4 min. At known irradiation time intervals, the samples (4 mL) are removed and, afterward, analysis is carried out by UV-visible (V) spectrophotometry (Ultrospec 2000, Biotech Pharmacia, Little Chalfont, UK) at 427 nm. A correlation based on linearity is laid down in the midst of the AY23 concentration, as well as the absorbance, which are in the range 0–50 mg/L holding a correlation coefficient,  $R^2 = 0.9981$ . Equation (1) is utilized in order to compute the photocatalytic eradication effectiveness ( $R$ , %) in the experiments:

$$R = \left( \frac{C_0 - C_t}{C_0} \right) \times 100, \quad (1)$$

such that,  $C_0$  (mg/mL) as well as  $C_t$  (mg/mL), are taken to be the primary concentration of AY23 and the concentration associated with AY23 at the duration  $t$ , respectively.

#### 3.3. Artificial Neural Network Method

In this paper, a three-layer feed-forward back propagation neural network is used for modeling the UV/ $\text{Ag-TiO}_2$  process (Figure 2). The input variables of the neural network are stated as initial concentration of dye (mg/L), UV light intensity ( $\text{W/m}^2$ ), initial dosage of nano  $\text{Ag-TiO}_2$  (mg/L), irradiation time (min). AY23 eradication percentage ( $R$ , %) is chosen as the experimental response or output variable.

The mean square error (MSE) is utilized as the error function. The MSE is computed from the predicted model, as well as real evaluated values associated with the response variable illustrated as below:

$$MSE = 1/N \sum_{j=1}^N (A_j - Y_j)^2, \quad (2)$$

in this case,  $A_j$  as well as  $Y_j$  are considered to be the predicted model and evaluated values related to the response variable, respectively,  $N$  is termed as the total number of data points.

Here, the feed-forward back propagation ANN model is laid down to forecast the eradication of AY23 in water. The transfer functions in the hidden layer are considered to be linear, as well as in

the output layer is taken to be log sigmoid. The gradient descent scheme has been used as a training algorithm. The gradient algorithm is susceptible to cumulative rounding errors and is suitable for long runs without an additional error-correction procedure. It is more robust in statistics, identification, and signal processing [7].

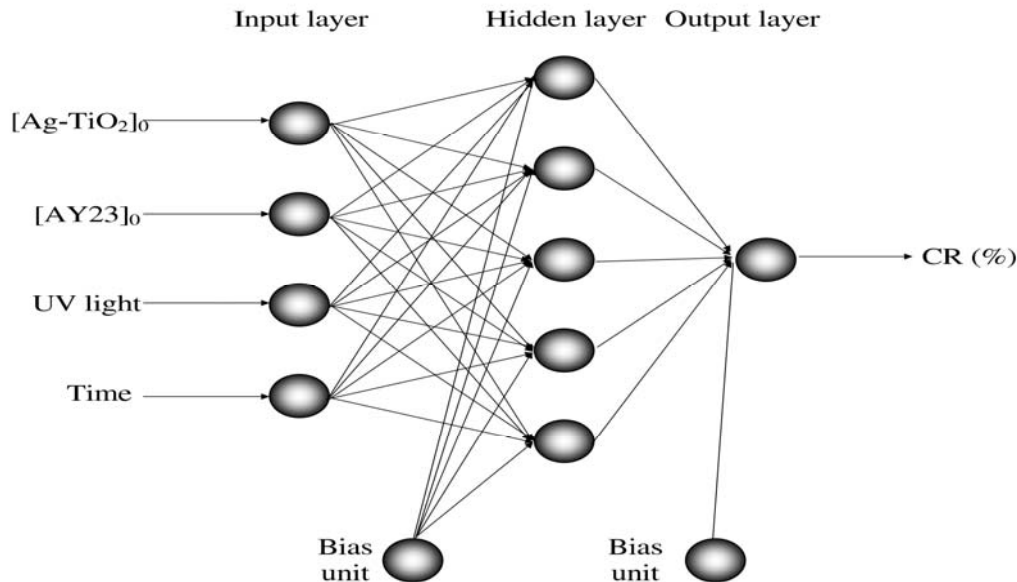


**Figure 2.** Schematic diagram of the artificial neural network (ANN) modeling approaches. CR: eradication percentage of AY23; UV light: ultraviolet light.

### 3.4. Imperialist Competitive Algorithm Method

The utilization of ICA in order to resolve various types of optimization problems is growing rapidly [26,27]. ICA has been used in different areas to be mentioned as sonar and radar, signal processing, and time series forecasting [28]. The ICA is suggested by Atashpaz et al. [16]. This technique is a novel socio-politically motivated global search scheme that is currently induced in order to deal with various optimization tasks. In [29], this algorithm is utilized to detect the optimized weights of the ANN. ICA has major performances to be mentioned, such as rapid convergence and superior global minimum attainment. The algorithm begins with choosing some arbitrary candidate solutions in the search space. These candidate solutions are termed as countries. The strength of each country is stated by the cost function related to the problem. Among these primary countries, few of them are chosen as imperialist on the basis of their strength. Every imperialist attempts to provide power to their country by improvising their colonies. This process in the final phase will lead the search towards the global optima.

In optimization problems, the ultimate intention is to extract an optimal solution on par with the variables related to the problem. Therefore, in these problems, an array of variables are generated which are needed to be optimized. In ICA, the term country is utilized for this array. In a  $N_{var}$ -dimensional optimization problem, a country is demonstrated by  $1 \times N_{var}$  array. This array is stated as below:

$$\text{Country} = [p_1, p_2, \dots, p_{N_{var}}], \quad (3)$$

where  $P_j : j = 1, 2, \dots, N_{var}$  are termed as the variables that need to be optimized.

The cost of a country is determined by analyzing the cost function at the variables  $(p_1, p_2, \dots, p_{N_{var}})$ . Hence:

$$\text{Cost} = f(\text{Country}) = f(p_1, p_2, \dots, p_{N_{var}}). \quad (4)$$

Here, the ICA model is initiated to forecast the eradication of AY23 in water by utilizing four operational variables denoted as estimators.

### 3.5. The Dataset

This investigation tries to generate the concept of the artificial intelligence on the basis of the predictive model for eradication of AY23 in water by utilizing a collection of chosen variables termed as the estimators. Datasets which are utilized to generate the ANN and ICA models in this paper are based on the laboratory studies performed under statistical experimental design [30]. Four parameters to be mentioned as primary dye concentration, UV light intensity, primary dosage of nano Ag-TiO<sub>2</sub>, as well as irradiation time are selected as the input variables and the eradication of AY23 as the output variable. The range of variables is summarized in Table 1.

**Table 1.** Range of studied variables.

Variable	Range
Input layer	
Ag-TiO <sub>2</sub> initial dosage (g/L)	0.01–0.05
AY23 initial concentration (mg/L)	5–60
UV light intensity (W/m <sup>2</sup> )	0–60
Irradiation time (min)	0–60
Output layer	
Removal of AY23 (%)	0–100

## 4. Models, Results, and Discussion

In this work, two different techniques, ANN and ICA have been applied in order to develop the predictive models for the eradication of AY23 in wastewater by implementing four operational variables, termed as the estimators.

### 4.1. Results and Discussion

Two different modeling methods, ANN and ICA, are utilized in order to develop the predictive models for the eradication of AY23 in wastewater by implementing the same set of estimators. Here various quantities of neurons are tested starting from two to 16, which are contained in the hidden layer. Each topology is iterated six times in order to forbid random correlation, taking into account the random initiation of the weights. Figure 3A, B state the relation between the network error and the number of neurons in the hidden layer in ANN and ICA models, respectively. It can be noticed that the performance of the network stabilized after the inclusion of an adequate number of hidden units, seven and six in the ANN and ICA models, respectively. The network which includes more neurons in the hidden layer cannot approach effectively the desired output.

The training and validation outcomes extracted from the ANN, along with the ICA model, are utilized to calculate several statistically-validated specifications to be mentioned as determination coefficient  $R^2$ , the root mean squared error (RMSE), the factor of accuracy  $A_f$ , as well as the Nash–Sutcliffe coefficient associated with the efficiency  $E_f$ . The chosen validated specifications are stated in the following form [31]:

$$R^2 = \left[ \frac{N \sum_{j=1}^N Y_j A_j - (\sum_{j=1}^N Y_j)(\sum_{j=1}^N A_j)}{\sqrt{[N \sum_{j=1}^N Y_j^2 - (\sum_{j=1}^N Y_j)^2] \times [N \sum_{j=1}^N A_j^2 - (\sum_{j=1}^N Y_j)^2]}} \right], \tag{5}$$

$$RMSE = \sqrt{\frac{\sum_{j=1}^N (A_j - Y_j)^2}{N}}, \tag{6}$$

$$A_f = 10^{\left(\frac{\sum_{j=1}^N \frac{|\log(\frac{A_j}{\bar{Y}})|}{N}\right)}, \tag{7}$$

$$E_f = 1 - \frac{\sum_{j=1}^N (A_j - Y_j)^2}{\sum_{j=1}^N (Y_j - \bar{Y})^2}, \tag{8}$$

where,  $\bar{Y}$  is termed to be the mean of the evaluated value related to the response variable. The coefficient of determination  $R^2$  exhibits the level of variability which is possible to be stated using the models, along with RMSE, which depicts the evaluation of the average error in forecasting related to the dependent variable. The preciseness factor  $A_f$ , a straightforward multiplicative factor exhibits the diffusion of outcomes around the forecast. A higher value of  $A_f$  will result in the minimal preciseness of the average estimation. The numerical value shows that there exists a flawless consent among all the forecasted and evaluated values [32]. The Nash-Sutcliffe coefficient of efficiency  $E_f$ , shows that the model fit is a generalized evaluation  $[-\infty; 1]$ , which compares the MSE produced with the help of a distinct simulated model to the variance of the target output sequence [33].

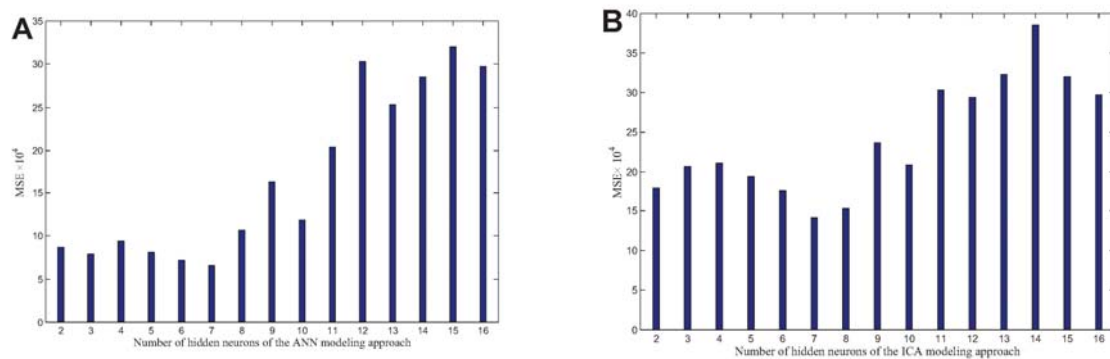


**Figure 3.** Implication of the quantity of neurons embedded in the hidden layer on the efficiency of the (A) ANN and (B) imperialist competitive algorithm (ICA) modeling schemes.

Considering both training and validation sets, the model forecasted and experimentally computed values of the withdrawal of AY23 in water are displayed in Figures 4 and 5, respectively. It distinctly reveals that the outcomes of the ANN scheme are in similar phase when compared with the corresponding experimental outcomes taking into consideration both cases, training (Figure 4A) and the validation sets (Figure 5A).

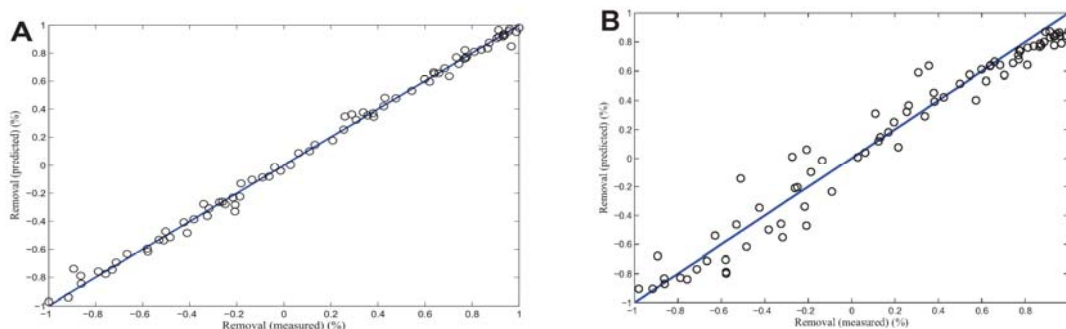


**Figure 4.** The measured and predicted eradication of AY23 in water using (A) ANN and (B) ICA schemes in training of the set based on the best optimum number of hidden layer neurons for the selected algorithms.

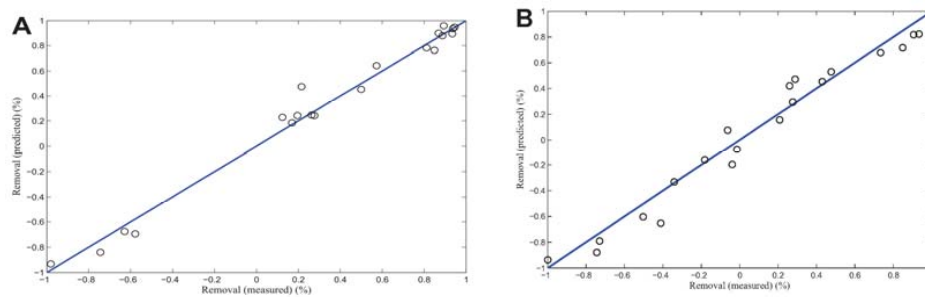


**Figure 5.** The measured and predicted eradication of AY23 in water using (A) ANN and (B) ICA schemes in validation of the set based on the best optimum number of hidden layer neurons for the selected algorithm.

Table 2 demonstrates the statistical comparison of the ANN and ICA models. The  $R^2$  value above 0.8 states that both the training and validation set are notably correlated. The  $A_f$  and  $E_f$  values are close to unity and the low RMSE affirms the superior extension and predictive capabilities of the two modeling techniques for the given dataset.

**Table 2.** Performance statistics of the ANN and ICA models.

Model	Sub-set	RMSE	$E_f$	$A_f$	$R^2$
ANN	Training	0.04039	1.01256	1.00103	1.00685
	Validation	0.08076	1.04562	0.99001	1.02212
ICA	Training	0.18345	0.95236	0.97852	0.94670
	Validation	0.19884	0.93545	0.94256	0.92575

RMSE: root mean squared error;  $E_f$ : Nash-Sutcliffe coefficient of the efficiency;  $A_f$ : factor of accuracy;  $R^2$ : determination coefficient.

The generated weights are listed in Tables 3 and 4 by gradient descent and ICA as training algorithms, respectively. Every weight decides what proportion of the incoming signal will be transferred into the neuron’s body [34].

**Table 3.** Matrices of weights by gradient descent as the training algorithm.

W1					W2		
Neuron	[Ag-TiO <sub>2</sub> ] <sub>0</sub>	[AY23] <sub>0</sub>	UV light	Time	Bias	Neuron	Weight
2	−0.082	3.940	14.211	1.286	9.752	2	−0.154
3	0.070	0.204	−0.092	0.221	−1.344	3	25.63
4	28.311	−15.42	−5.464	−13.37	−20.03	4	−0.108
5	−2.917	2.188	−2.978	0.235	−0.657	5	−0.270
6	3.043	1.473	2.946	2.971	1.648	6	0.292
7	−0.374	1.921	1.376	2.425	−3.305	7	−0.758
						Bias	21.27

W1: weights between input and hidden layers; W2: weights between hidden and output layers.

**Table 4.** Matrices of weights by ICA as the training algorithm.

W1					W2		
Neuron	[Ag-TiO <sub>2</sub> ] <sub>0</sub>	[AY23] <sub>0</sub>	UV light	Time	Bias	Neuron	Weight
2	−0.258	−0.824	0.999	−0.712	−0.979	2	0.341
3	0.003	−0.864	−0.483	0.726	0.775	3	0.382
4	−0.799	−0.347	0.081	−0.596	−0.043	4	−0.879
5	−0.651	−0.210	−0.667	0.189	−0.466	5	−0.514
6	−0.448	0.465	−0.994	−0.369	−0.161	6	−0.899
						Bias	−0.803

The neural network weight matrix is utilized in order to evaluate the relative importance of the multiple input variables on the output variables. An equation on the basis of the partitioning of connection weights is stated as follows [35]:

$$I_j = \frac{\sum_{m=1}^{m=N_h} \left( \left( |W_{jm}^{ih}| / \sum_{k=1}^{N_i} |W_{km}^{ih}| \right) \times |W_{mn}^{ho}| \right)}{\sum_{k=1}^{k=N_i} \left\{ \sum_{m=1}^{m=N_h} \left( \left( |W_{jm}^{ih}| / \sum_{k=1}^{N_i} |W_{km}^{ih}| \right) \times |W_{mn}^{ho}| \right) \right\}}, \quad (9)$$

where  $I_j$  is termed as the relative significance of the  $j$ th input variable on the output variable.  $W_S$  are termed as the connection weights.  $N_i$  and  $N_h$  are the numbers of inputs, and hidden neurons, respectively. The superscripts  $i$ ,  $h$ , and  $o$  signify the input, hidden, and output layers, respectively. Subscripts  $k$ ,  $m$  and  $n$  signify the input, hidden, and as output neurons, respectively.

The relative importance of input variables on the AY23 removal efficiency is exhibited in Table 5. It can be noticed that all variables have influences on the AY23 removal efficiency. However, the influence of AY23 initial concentration in comparison with others is greater. Thus, none of the variables investigated in this paper could be neglected in the present analysis.

**Table 5.** Relative importance (%) of input variables on acid yellow 23 (AY23) removal efficiency.

Input Variable	Importance (%)
Ag-TiO <sub>2</sub> initial dosage (g/L)	10
AY23 initial concentration (mg/L)	40
UV light intensity (W/m <sup>2</sup> )	30
Time (min)	20

## 5. Concluding Remarks

In this paper, the withdrawal of AY23 by utilization of the UV/Ag-TiO<sub>2</sub> operation is researched. Predictive and universalization abilities of the ANN and ICA models in order to eliminate the AY23 in water are investigated by the implementation of a statistically-designed dataset gathered from the literature. The initial concentration of dye, UV light intensity, initial dosage, of nano Ag-TiO<sub>2</sub>, as well as irradiation time, are utilized as predictor variables.

The elimination of AY23 is successfully forecasted by implementing a three-layer neural network with seven neurons in the hidden layer in the ANN model, as well as by implementing a three-layer neural network with six neurons in the hidden layer in the ICA model. A comparison of the predictive performances of the ANN and ICA models is carried out by utilizing the statistical criteria of RMSE,  $R^2$ ,  $A_f$ , and  $E_f$ . Both ANN and ICA modeling methods display good prediction in this work. The ANN model is more precise when compared with ICA model. The optimum conditions, as well as the relative variable importance for each variable on the AY23 removal efficiency are represented. This paper has a significant contribution in initializing a superior starting point for the removal of AY23 in water by the UV/Ag-TiO<sub>2</sub> process. As the progress of artificial intelligence methodologies have been affected significantly by a deficiency of training techniques, it is taken into consideration that our schemes cover up this emptiness, and it is our hope that they will result in several new applications.

**Author Contributions:** All authors contributed equally to this work. All authors read and approve the final manuscript.

**Conflicts of Interest:** The authors declare no conflict of interest.

## References

- Behnajady, M.A.; Modirshahla, N.; Ghanbary, F. A kinetic model for the decolorization of C.I. Acid Yellow 23 by Fenton process. *J. Hazard. Mater.* **2007**, *148*, 98–102. [[CrossRef](#)] [[PubMed](#)]

2. Castro, A.L.; Nunes, M.R.; Carvalho, A.P.; Costa, F.M.; Floreencio, M.H. Synthesis of anatase TiO<sub>2</sub> nanoparticles with high temperature, stability and photocatalytic activity. *Solid State Sci.* **2008**, *10*, 602–606. [[CrossRef](#)]
3. Bagheri, A.R.; Ghaedi, M.; Hajati, S.; Ghaedi, A.M.; Goudarzi, A.; Asfaram, A. Random forest model for the ultrasonic-assisted removal of chrysoidine G by copper sulfide nanoparticles loaded on activated carbon; response surface methodology approach. *RSC Adv.* **2015**, *5*, 59335–59343. [[CrossRef](#)]
4. Chang, Y.; Erera, A.L.; White, C.C. Risk assessment of deliberate contamination of food production facilities. *IEEE Trans. Syst. Man Cybern. Syst.* **2015**, *47*, 381–393. [[CrossRef](#)]
5. Dil, E.A.; Ghaedi, M.; Asfaram, A.; Hajati, S.; Mehrabi, F.; Goudarzi, A. Preparation of nanomaterials for the ultrasound-enhanced removal of Pb<sup>2+</sup> ions and malachite green dye: Chemometric optimization and modeling. *Ultrason. Sonochem.* **2017**, *34*, 677–691. [[CrossRef](#)] [[PubMed](#)]
6. Fan, C.T.; Wang, Y.K.; Huang, C.R. Heterogeneous information fusion and visualization for a large-scale intelligent video surveillance system. *IEEE Trans. Syst. Man Cybern. Syst.* **2016**, *47*, 593–604. [[CrossRef](#)]
7. Jafari, R.; Yu, W. Fuzzy Control for Uncertainty Nonlinear Systems with Dual Fuzzy Equations. *J. Intell. Fuzzy. Syst.* **2015**, *29*, 1229–1240. [[CrossRef](#)]
8. Jafari, R.; Yu, W. Fuzzy Differential Equation for Nonlinear System Modeling with Bernstein Neural Networks. *IEEE Access* **2017**, *4*, 9428–9436. [[CrossRef](#)]
9. Jafari, R.; Yu, W. Uncertainty Nonlinear Systems Modeling with Fuzzy Equations. *Math. Probl. Eng.* **2017**, *2017*. [[CrossRef](#)]
10. Jafarian, A.; Jafari, R.; Khalili, A.; Baleanud, D. Solving fully fuzzy polynomials using feed-back neural networks. *Int. J. Comp. Math.* **2015**, *92*, 742–755. [[CrossRef](#)]
11. Khataee, A.R. Photocatalytic removal of C.I. Basic Red 46 on immobilized TiO<sub>2</sub> nanoparticles: Artificial neural network modeling. *Environ. Technol.* **2009**, *30*, 1155–1168. [[CrossRef](#)] [[PubMed](#)]
12. Shirvani Ardekani, P.; Karimi, H.; Ghaedi, M.; Asfaram, A.; Kumar Purkait, M. Ultrasonic assisted removal of methylene blue on ultrasonically synthesized zinc hydroxide nanoparticles on activated carbon prepared from wood of cherry tree: Experimental design methodology and artificial neural network. *J. Mol. Liq.* **2017**, *229*, 114–124. [[CrossRef](#)]
13. Kunwar, P.; Shikha, G. Artificial intelligence based modeling for predicting the disinfection by-products in water. *Chemom. Intell. Lab. Syst.* **2012**, *114*, 122–131.
14. Niknam, T.; Taherian Fard, E.; Pourjafarian, N.; Roustaa, A. An efficient hybrid algorithm based on modified imperialist competitive algorithm and K-means for data clustering. *Eng. Appl. Artif. Intell.* **2011**, *24*, 306–317. [[CrossRef](#)]
15. Yousefi, M.; Darus, A.N.; Mohammadi, H. An imperialist competitive algorithm for optimal design of plate-fin heat exchangers. *Int. J. Heat Mass Transf.* **2012**, *55*, 3178–3185. [[CrossRef](#)]
16. Atashpaz-Gargari, E.; Lucas, C. Imperialist competitive algorithm: An algorithm for optimization inspired by imperialistic competition. In Proceedings of the IEEE Congress on Evolutionary Computation, Singapore, 25–28 September 2007; pp. 4661–4667.
17. Khajeh, M.; Kaykhahi, M.; Sharafi, A. Application of PSO-artificial neural network and response surface methodology for removal of methylene blue using silver nanoparticles from water sample. *J. Ind. Eng. Chem.* **2013**, *19*, 1624–1630. [[CrossRef](#)]
18. Wang, H.W.; Lin, H.C.; Kuo, C.H.; Cheng, Y.L.; Yeh, Y.C. Synthesis and photocatalysis of mesoporous anatase TiO<sub>2</sub> powders incorporated Ag nanoparticles. *J. Phys. Chem. Solids* **2008**, *69*, 633–635. [[CrossRef](#)]
19. Behnajady, M.A.; Modirshahla, N.; Daneshvar, N.; Rabbani, M. Photocatalytic degradation of an azo dye in a tubular continuous-flow photoreactor with immobilized TiO<sub>2</sub> on glass plates. *J. Chem. Eng.* **2007**, *127*, 167–176. [[CrossRef](#)]
20. Mazaheri, H.; Ghaedi, M.; Ahmadi Azqhandi, M.H.; Asfaram, A. Application of machine/statistical learning, artificial intelligence and statistical experimental design for the modeling and optimization of methylene blue and Cd(II) removal from a binary aqueous solution by natural walnut carbon. *Phys. Chem. Chem. Phys.* **2017**, *19*, 11299–11317. [[CrossRef](#)] [[PubMed](#)]
21. Asfaram, A.; Ghaedi, M.; Ahmadi Azqhandi, M.H.; Goudarzi, A.; Dastkhooon, M. Statistical experimental design, least squares-support vector machine (LS-SVM) and artificial neural network (ANN) methods for modeling the facilitated adsorption of methylene blue dye. *RSC Adv.* **2016**, *6*, 40502–40516. [[CrossRef](#)]

22. Asfaram, A.; Ghaedi, M.; Hajati, S.; Goudarzi, A. Ternary dye adsorption onto MnO<sub>2</sub> nanoparticle-loaded activated carbon: derivative spectrophotometry and modeling. *RSC Adv.* **2015**, *5*, 72300–72320. [[CrossRef](#)]
23. Asfaram, A.; Ghaedi, M.; Hajati, S.; Goudarzi, A. Synthesis of magnetic  $\gamma$ -Fe<sub>2</sub>O<sub>3</sub>-based nanomaterial for ultrasonic assisted dyes adsorption: Modeling and optimization. *Ultrason. Sonochem.* **2016**, *32*, 418–431. [[CrossRef](#)] [[PubMed](#)]
24. Bagheri, A.R.; Ghaedi, M.; Asfaram, A.; Hajati, S.; Ghaedi, A.M.; Bazrafshan, A. Modeling and optimization of simultaneous removal of ternary dyes onto copper sulfide nanoparticles loaded on activated carbon using second-derivative spectrophotometry. *J. Taiwan Inst. Chem. Eng.* **2016**, *65*, 212–224. [[CrossRef](#)]
25. Azad, F.N.; Ghaedi, M.; Asfaram, A.; Jamshidi, A.; Hassani, G.; Goudarzi, A. Optimization of the process parameters for the adsorption of ternary dyes by Ni doped FeO (OH)-NWsAC using response surface methodology and an artificial neural network. *RSC Adv.* **2016**, *6*, 19768–19779. [[CrossRef](#)]
26. Chen, C.L.P.; Zhang, T.; Tam, S.C. A novel evolutionary algorithm solving optimization problems. In Proceedings of the IEEE International Conference on Systems, Man, and Cybernetics, San Diego, CA, USA, 5–8 October 2014.
27. Puntonet, C.G.; Grriz, J.M.; Salmern, M.; Hornillo-Mellado, S. Theoretical method for solving BSS-ICA using SVM. In Proceedings of the International Conference on Independent Component Analysis and Signal Separation, Granada, Spain, 22–24 September 2004; pp. 256–262.
28. Gorriz, J.M.; Puntonet, C.G.; Salmeron, M.; Ortega, J. New method for filtered ICA signals applied to volatile time series. In Proceedings of the 7th International Work Conference on Artificial and Natural Neural Networks IWANN 2003 Lecture Notes in Computer Science, Menorca, Spain, 3–6 June 2003; Volume 2687, pp. 433–440.
29. Pothiya, S.; Ngamroo, I.; Kongprawechnon, W. Application of multiple tabu search algorithm to solve dynamic economic dispatch considering generator constraints. *Energy Convers. Manag.* **2008**, *49*, 506–516. [[CrossRef](#)]
30. Ghanbary, F.; Jafarian, A. Preparation and photocatalytic properties of silver doped titanium dioxide nanoparticles and using artificial neural network for modeling of photocatalytic activity. *J. Basic Appl. Sci.* **2012**, *12*, 2889–2898.
31. Karul, C.; Soyupak, S.; Clesiz, A.F.; Akbay, N.; German, E. Case studies on the use of neural networks in eutrophication modeling. *Ecol. Model.* **2000**, *134*, 145–152. [[CrossRef](#)]
32. Smith, G.N. *Probability and Statistics in Civil Engineering*; Collins: London, UK, 1986.
33. Nash, J.E.; Sutcliffe, I.V. River flow forecasting through conceptual models Part I—A discussion of principles. *J. Hydrol.* **1970**, *10*, 282–290. [[CrossRef](#)]
34. Slokar, Y.M.; Zupan, J.; Marechal, A.M.L. The use of artificial neural network (ANN) for modeling of the H<sub>2</sub>O<sub>2</sub>/UV decoloration process. *Dyes Pigment* **1999**, *42*, 123–135. [[CrossRef](#)]
35. Aleboyeh, A.; Kasiri, M.B.; Olya, M.E.; Aleboyeh, H. Prediction of azo dye decolorization by UV/H<sub>2</sub>O<sub>2</sub> using artificial neural networks. *Dyes Pigment* **2008**, *77*, 288–294. [[CrossRef](#)]

